https://doi.org/10.5194/egusphere-2024-1306
Preprint. Discussion started: 22 May 2024
© Author(s) 2024. CC BY 4.0 License.

Revised conceptual model of the Solfatara magmatic-hydrothermal system (Campi Flegrei, Italy), time changes during the last 40 years, and prediction of future scenarios

Luigi Marini[1], Claudia Principe[2,3], Matteo Lelli[2,4]

[1] STEAM srl, Pisa, I-56121, Italy
[2] CNR, Istituto di Geoscienze e Georisorse, Pisa, I-56124, Italy
[3] INGV - Istituto Nazionale di Geofisica e Vulcanologia, Osservatorio Vesuviano, Napoli, I-80124, Italy
[4] INGV - Istituto Nazionale di Geofisica e Vulcanologia, Sezione di Pisa, Pisa, I-56125, Italy

Correspondence to: Matteo Lelli (m.lelli@igg.cnr.it)

Abstract. We revised the conceptual model of the Solfatara magmatic-hydrothermal system based on the results of new gas-geoindicators (Marini et al., 2022) and the available geological, volcanological, and geophysical information from surface surveys and deep geothermal wells. Using the new gas-geoindicators, we monitored the temperature and total fluid pressure over a time interval of ~40 years: (i) in the shallow reservoir (0.25-0.45 km depth), where CO equilibrates; (ii) in the intermediate reservoir (2.7-4.0 km depth), where CH_4 attains equilibrium; (iii) in the deep reservoir (6.5-7.5 km depth), where H_2S achieves equilibrium. From 1983 to 2022, the temperature and total fluid pressure of the shallow reservoir did not depart significantly from ~220°C and ~25 bar, whereas remarkable, progressive increments in temperature and total fluid pressure occurred in the intermediate and deep reservoirs, with peak values of 590-620 °C and 1200-1400 bar in the intermediate reservoir and 1010-1040°C and 3000-3200 bar in the deep reservoir, in 2020. The revised conceptual model allowed us to explain the evolution of: (a) pressurization-depressurization in the intermediate reservoir, acting as the "engine" of bradyseism, (b) time changes of total fluid pressure in the deep reservoir, working as the "on-off switch" of magmatic degassing. We also used the revised conceptual model to predict possible future scenarios in the lack of external factors.

1 Introduction

The Campi Flegrei, Phlegraean Fields in English, are located next to Naples (Fig. 1a), are a very densely populated area with about 500,000 inhabitants, and are considered to be one of the most dangerous volcanic sites worldwide, as they were impacted by several large-scale explosive eruptions. Slow vertical ground movements known as "bradyseism" have affected the Campi Flegrei area since at least Roman times with alternating episodes of uplift or resurgence and deflation or subsidence (Lyell, 1830). The slow ground movements typical of the bradyseism are totally different from (and should not be confused with) the fast and local uplift preceding the last volcanic eruption in the Campi Flegrei area that began on 29 September 1538, had the duration of a week, and consisted in a small phreatomagmatic event generating the Monte Nuovo cone (Guidoboni and Ciuccarelli, 2011). The last resurgence cycle begun in 1950, caused maximum uplifts of 1.77 m in 1969-1972 and 1.79 m in

https://doi.org/10.5194/egusphere-2024-1306
Preprint. Discussion started: 22 May 2024
© Author(s) 2024. CC BY 4.0 License.

1982-1984, both followed by deflation periods, the last of which ended in 2005, when the still ongoing inflation phase started (Del Gaudio et al., 2010; De Martino et al., 2014; Tramelli et al., 2021). Ground deformation was accompanied by seismicity (e.g., D'Auria et al., 2011; Di Luccio et al., 2015) and changes in the chemistry and emission rate of the fumarolic fluids released from Solfatara-Pisciarelli (Buono et al., 2023 and references therein; Fig. 1b), the most impressive manifestations in the Campi Flegrei.

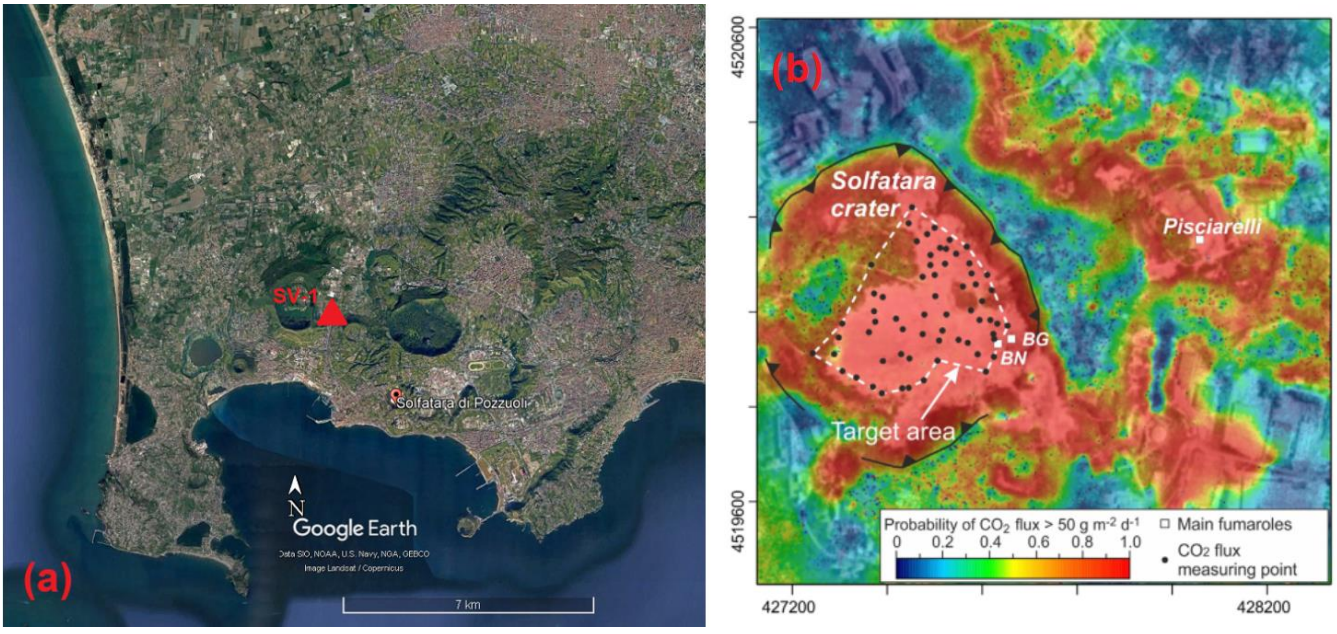

Figure 1: (a) © Google-Earth image of Campi Flegrei, showing the location of the deep geothermal well San Vito 1 (SV-1). (b) Map of the Solfatara-Pisciarelli diffuse degassing structure elaborated from the 1998-2016 dataset of CO_2 fluxes also showing the location of the Bocca Grande (BG), Bocca Nuova (BN), and Pisciarelli (Pi) fumarolic vents (from Chiodini et al., 2021; Elsevier licence number 5601960223358 on Aug 04, 2023).

The Solfatara edifice has a sub-circular crater, with a diameter varying between 610 and 710 m and an area of ~0.35 km^2 (Isaia et al., 2015). It was generated by a purely hydrothermal event (Principe, 2024) which possibly occurred about 4200-4400 ka BP (Isaia et al., 2009). The morphology of the Solfatara edifice and crater as well as the upflow of deep fluids are mainly controlled by Apenninic and anti-Apenninic tectonic elements, striking WNW and ENE, respectively (Rosi and Sbrana, 1987). During the last 40 years, the Solfatara fumarolic fluids were periodically collected and analyzed, in the framework of the Campi Flegrei volcanic surveillance (Chiodini et al., 2021 and references therein; Buono et al., 2023). Fluids samples were mainly obtained from the Solfatara vents known as Bocca Grande and Bocca Nuova, discharging CO_2-rich superheated steam, with smaller amounts of H_2S, N_2, H_2, CH_4, He, CO, and Ar, in decreasing order, at outlet temperatures of 150-165°C and 135-154°C, respectively. Thus, a very large geochemical database, one of the longest record series worldwide, was produced. It comprises the chemical concentrations of several gas species in fumarolic fluids (Table S1) and a congruous number of isotopic data (Marini et al., 2022 and references therein).

https://doi.org/10.5194/egusphere-2024-1306
Preprint. Discussion started: 22 May 2024
© Author(s) 2024. CC BY 4.0 License.

A fundamental tool to understand the behaviour of the system of interest and predict its future evolution and scenarios is the conceptual model elaborated merging available scientific data, in the framework of the general conceptual model of volcano-hosted magmatic-hydrothermal systems of Fournier (1999; see section 4.4), and following the guidelines of Cumming (2009, 2016) for the hydrothermal domain. The conceptual models proposed so far for the Solfatara magmatic-hydrothermal system extend to depths of a few hundred meters (Cioni et al., 1984) or 2.5-3.0 km (Caliro et al., 2007) and refer to the hydrothermal domain. In fact, the gas equilibration temperatures and pressures obtained in previous studies by Cioni and coworkers and Chiodini and coworkers were exclusively or chiefly based on geothermometers and geobarometers controlled entirely or mostly by CO, which equilibrates at shallow depth. Among the other gas species, CH_4 was considered together with CO in some cases, erroneously assuming it has little effects on the obtained results (see section 4.3), or treated as a tracer rather than an indicator, whereas H_2S was considered a gas species of little interest based on the behaviour of the Giggenbach's gas-geothermometer involving pyrite (Caliro et al., 2007).

Recently, we proposed new gas geothermometers and geobarometers, which were suitably calibrated for different plausible expansion paths of the Solfatara fluids, also considering the deviations from the ideal gas behaviour, for the first time. Our results were presented and thoroughly discussed by Marini et al. (2022). In this work, we summarize the main findings of Marini et al. (2022), taking into account the last data produced by Buono et al. (2023) for Bocca Grande and Bocca Nuova fumaroles for October 2020 to January 2022. Moreover, in this work, we use our geothermometric and geobarometric results, as well as the information from other disciplines (e.g., surface geo-volcanological surveys, data from geothermal deep wells, and geophysical investigations) to elaborate a revised conceptual model of the Solfatara magmatic-hydrothermal system which extends at magmatic depths (~8 km) and represents a considerable step forward with respect to previous conceptual models. Finally, in this work, we show that our revised conceptual model explains the slow vertical ground movements and other active processes typical of the bradyseism, and we use it to predict future scenarios.

The reason that pushed us to write this paper is to provide a contribution to the discussion animating, in this period, the international scientific community on the possible evolution of the unrest episode currently affecting the Campi Flegrei. The mitigation of the volcanic hazard in the Campi Flegrei is not a local issue because worldwide volcanologists look at it as an analogue of similar volcanic systems (see Chapter 11 of Marini et al., 2022).

2 Methods

Three distinct equilibrium temperatures and related total fluid pressures were computed. The first one refers to CO equilibrium, which is controlled by the homogeneous reaction:

$$CO_2 + H_2 = CO + H_2O. \quad (1)$$

The second one relates to CH_4 equilibrium, which is governed by the homogeneous reaction:

$$CO_2 + 4\,H_2 = CH_4 + 2\,H_2O. \quad (2)$$

The third one refers to H_2S equilibrium, which is ruled by the heterogeneous reaction:

https://doi.org/10.5194/egusphere-2024-1306
Preprint. Discussion started: 22 May 2024
© Author(s) 2024. CC BY 4.0 License.

$$CaSO_{4(s)} + CO_2 + 4\ H_2 = CaCO_{3(s)} + H_2S + 3\ H_2O, \quad (3)$$

involving anhydrite [$CaSO_{4(s)}$] and calcite [$CaCO_{3(s)}$]. Of interest is also the heterogeneous redox reaction:

$$CaSO_{4(s)} + CH_4 = CaCO_{3(s)} + H_2S + H_2O. \quad (4)$$

which is assumed to fix CH_4 concentration in the zone of H_2S equilibration. The CO and CH_4 equilibrium temperatures and total fluid pressures were computed for the saturation decompression path of Solfatara fluids involving a brine containing 21 wt% NaCl, assuming gas equilibration in a single saturated vapor phase. The H_2S equilibrium temperature and total fluid pressures, as well as the CH_4 concentration in the H_2S equilibration zone, were calculated for the saturation decompression path of Solfatara fluids involving a brine containing 33.5 wt% NaCl, assuming gas equilibration in a single saturated vapor phase. Equilibrium temperatures and related total fluid pressures are reported in Table S1.

3 Results

The computed CO-, CH_4- and H_2S equilibrium temperatures are shown in Fig. 2 for all the gas samples collected from both Bocca Grande, from June 1983 to January 2022, and Bocca Nuova, from March 1995 to January 2022 (data from Buono et al., 2023 and references therein). The corresponding total fluid pressures are displayed in Fig. 3. To facilitate the comparison between numbers, the CO-, CH_4- and H_2S equilibrium temperatures and related total fluid pressures calculated for Bocca Grande were subdivided in 24 discrete time intervals and the average and standard deviation for each time interval were computed and reported in Tables A1 and A2. The following observations can be drawn from Figs. 2 and 3 and Tables A1 and A2:

(i) Reaction (1) indicates low and nearly constant CO-equilibrium temperature and total fluid pressure from 1983 to 2022, 217±9°C, 24.5±4.0 bar, for Bocca Grande, and 219±6°C, 25.4±2.9 bar, for Bocca Nuova[1].

(ii) In contrast, the CH_4-equilibrium temperature and total fluid pressure obtained from reaction (2) increase gradually and significantly with time, from 246±8°C, 38.5±5.6 bar in June 1983-July 1984 to 589±8°C, 1226±46 bar in 2020, for Bocca Grande, and attained 622±12°C, 1401±68 bar in 2020, for Bocca Nuova. Slightly lower values are estimated for the samples collected in 2021-2022, namely, 580±8°C, 1186±52 bar, for Bocca Grande, and 615±9°C, 1350±54 bar, for Bocca Nuova. Nevertheless, the 2020 values compare with those of 2021-2022 considering short-time changes.

(iii) The H_2S-equilibrium temperature and total fluid pressure related to reaction (3) experienced a progressive and considerable increment with time as well, from 667±24°C, 1308±102 bar in June 1983-July 1984 to 1010±14°C, 3039±73 bar in 2020, at Bocca Grande, and achieved 1039±25°C, 3162±129 bar in 2020, at Bocca Nuova. Weakly smaller values are obtained for the samples collected in 2021-2022, namely, 975±23°C, 2901±120 bar, for Bocca Grande, and 1008±20°C, 3012±97 bar, for Bocca Nuova. Nevertheless, the 2020 values overlap those of 2021-2022 taking into account short-time variations.

[1] Somewhat higher temperatures were computed for the 2010-2021 period by Chiodini et al. (2021) using the CO/CO_2 geothermometer and the redox buffers of either D'Amore and Panichi (1980) or that of the Campanian Volcanoes (Chiodini and Marini, 1998) 218-267°C and 27-60 bar and 238-287°C and 37-78 bar, respectively.

https://doi.org/10.5194/egusphere-2024-1306
Preprint. Discussion started: 22 May 2024
© Author(s) 2024. CC BY 4.0 License.

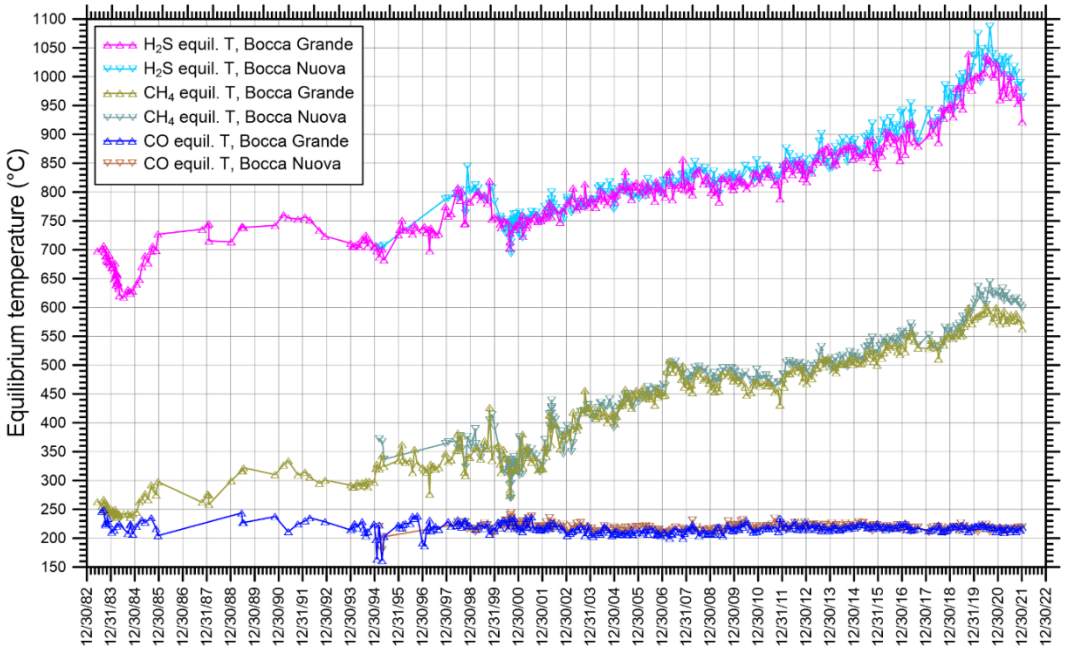

Figure 2: Chronogram of CO-, CH_4- and H_2S equilibrium temperatures for Bocca Grande, from June 1983 to January 2022, and from Bocca Nuova, from March 1995 to January 2022, calculated from the data of Cioni and coworkers and Chiodini and coworkers (Buono et al., 2023 and references therein).

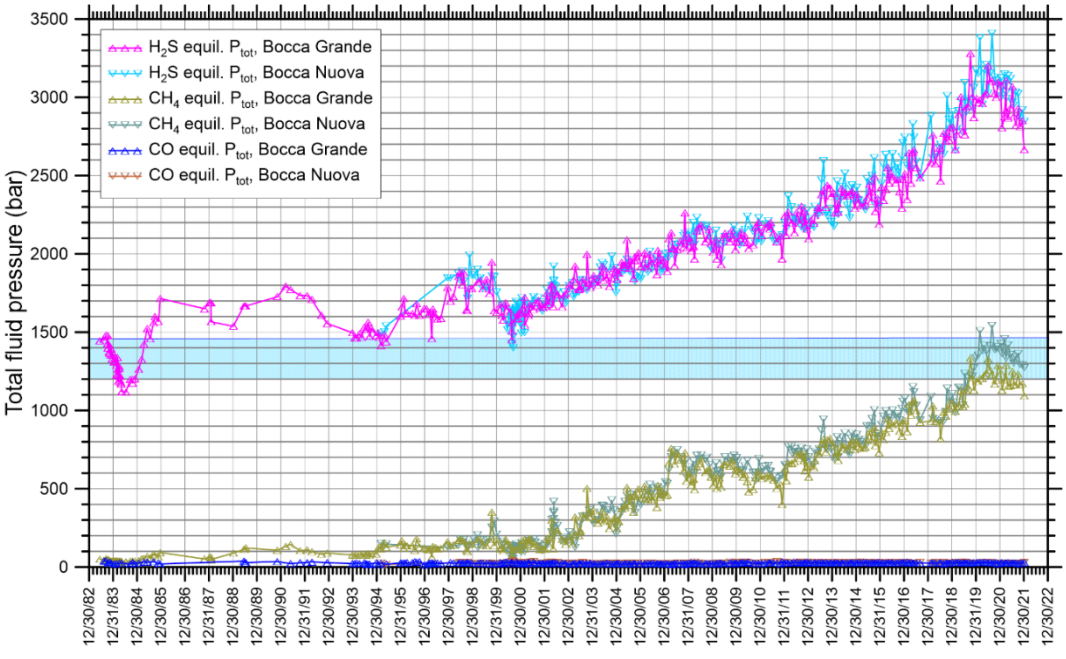

Figure 3. Chronogram of CO-, CH_4- and H_2S total fluid pressures for Bocca Grande, from June 1983 to January 2022, and for Bocca Nuova, from March 1995 to January 2022, calculated from the data of Cioni and coworkers and Chiodini and coworkers (Buono et al., 2023 and references therein). The strip of sky-blue colour indicates the external pressure expected at a depth of 6.5 – 7.5 km, where reaction (3) is assumed to attain the equilibrium condition.

https://doi.org/10.5194/egusphere-2024-1306
Preprint. Discussion started: 22 May 2024
© Author(s) 2024. CC BY 4.0 License.

4 Discussion

4.1 Noteworthy geo-volcanological aspects and findings of deep geothermal wells

The Campi Flegrei are within the Campanian Plain, a Neogene tectonic graben filled by a sequence of clastic and volcanoclastic sediments and volcanic rocks covering the Mesozoic carbonate basement which has been lowered to depths of some kilometres (Cassano and La Torre, 1987; Zollo et al., 2008). At least two large-scale explosive eruptions occurred in the Campi Flegrei. The most important one, known as Campanian Ignimbrite (CI) eruption, occurred 39.85 ± 0.14 ka BP (Giaccio et al., 2017), and generated either a single caldera (e.g., Rosi et al., 1983) or a nested caldera (e.g., Barberi et al., 1991; Acocella, 2008). The second most significant eruption is known as Neapolitan Yellow Tuff (NYT) eruption, occurred 14.9 ± 0.4 ka BP (Deino et al., 2004) from several vents and either reactivated both compartments of the nested CI caldera (e.g., Acocella, 2008) or reactivated the inner CI caldera (e.g., Barberi et al., 1991) or produced a new caldera (e.g., Lirer et al., 1987). In the time span between the CI and the NYT eruptions, volcanic activity was submarine, whereas the post-NYT activity was mainly subaerial (Rosi et al., 1983).

The early inference of Rittmann (1950) on the occurrence of a large caldera collapse in the Campi Flegrei was confirmed by the volcano-stratigraphic and structural investigations of Rosi et al., (1983) who recognized that the Campi Flegrei caldera formed as a consequence of the CI eruption, described the geological evolution of Campi Flegrei and, *inter alias*, mapped the caldera rim portions identifiable in the field (see also the "Geological and gravimetric map of Phlegrean Fields at the 1:15,000 scale" of Principe et al., 1987). A few years later, Lirer et al., (1987) recognized a smaller caldera which they attributed to the NYT eruption. A remarkable step forward was made by Barberi et al. (1991) who carried out a synthesis work by merging gravimetric and aeromagnetic data, both on-land and offshore, with the findings of surface geological and volcanological surveys and those of the deep geothermal wells drilled by AGIP-ENEL in the '70s and '80s. In this way, they redefined the geometry of both the outer and inner calderas, suggesting that both were produced as a direct consequence of the CI eruption. In more detail, according to Barberi et al. (1991): (i) the outer caldera rim (the southern portion of which was reconstructed based on offshore data) is indicated by the outer series of gravity highs (Fig. 4) distributed along a subcircular structure of ~ 13 km in diameter, whereas (ii) the inner caldera rim is marked by the inner circular belt of gravity highs and delimits a more collapsed central zone of ~11-12 km in diameter with a total drop of ~1.6 km. A circular sector of ~1-2 km in width (increasing northwards) and 0.7-0.8 km as maximum drop separates the inner caldera structure from the outer one.

The gravimetric low present in the central part of the Bouguer anomaly map of Fig. 4, coinciding with the inner caldera block, deserves further attention because it is circumscribed by the boundary of vertical ground movements computed by Bevilaqua et al. (2020) applying the Radial Interpolation Method to real geodetic data collected at the Campi Flegrei caldera in selected time intervals during the last 39 years. The implication is that ground deformation affects the inner caldera block only. The gravimetric low may be controlled by different factors, such as: (i) the high thickness of the low-density pyroclastic filling, (ii) the lack of dense lava bodies, (iii) the lowering of the isotherms and of the iso-density lines related to the hydrothermal circulation, and (iv) the greater depth of the thermometamorphic complex (Barberi et al., 1991). Nevertheless, considering that

https://doi.org/10.5194/egusphere-2024-1306
Preprint. Discussion started: 22 May 2024
© Author(s) 2024. CC BY 4.0 License.

the circular-shaped gravity minimum corresponds with the area affected by ground movements and accepting the hypothesis that ground deformation is controlled by pressurization-depressurization of a supercritical[2] gas phase, mainly constituted by H_2O and CO_2, which saturates the pore spaces of a relatively deep reservoir covered by a caprock, as recognized in several geophysical studies (see section 4.4), we propose that gas saturation is the cause or the main contributing cause of the decrease in density and gravity.

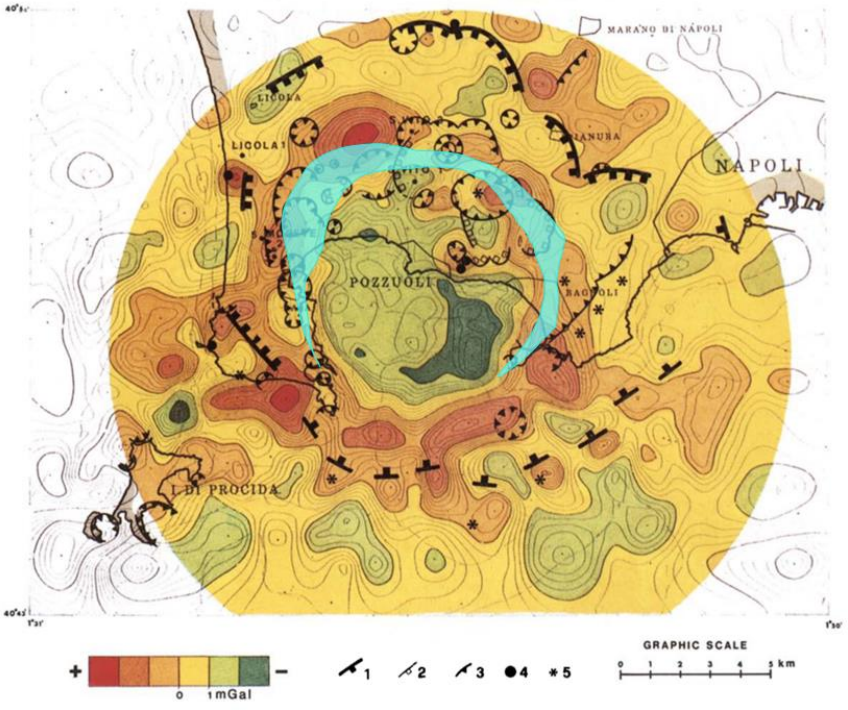

Figure 4. Map of Bouguer anomaly high-pass filter, based on 770 ground and 500 sea-bottom homogeneously distributed gravity stations (measurements by the Italian Geological Survey and AGIP), with a mean density of ~ 5 stations per km^2 (from Barberi et al., 1991, modified; Elsevier licence number 5601951169171 on Aug 04, 2023). Also shown are volcanic structures (1=caldera rim; 2=minor, post NYT, volcano tectonic collapsed areas; 3=crater rim; 4=lava dome; 5=eruptive centre) and the boundary of vertical ground movement computed by Bevilaqua et al. (2020; area of cyan colour). The Solfatara is the crater immediately to the east of Pozzuoli.

The occurrence of a gas-saturated relatively deep reservoir is supported by the findings of the vertical geothermal well San Vito 1 (SV-1 for short), which is located within the area of the gravimetric low and ground deformation (Fig. 4). The SV-1 geothermal well was drilled by AGIP-ENEL in the early '80s and reached a total depth of 3046 m, where a temperature >419°C was estimated to be present (Bruni et al., 1985). At depths of 2500-2800 m b.g.l. and temperatures of 360-385°C, the SV-1 geothermal well encountered a level of altered rocks with abundant hydrothermal quartz (Chelini and Sbrana, 1987). The first short-term production test of well SV-1 was ended by killing the well due to the rapid temperature increase at the well head,

[2] The adjective supercritical is used to indicate temperatures and pressures higher than those of the critical point of pure water, i.e., 374 °C and 222 bar.

https://doi.org/10.5194/egusphere-2024-1306
Preprint. Discussion started: 22 May 2024
© Author(s) 2024. CC BY 4.0 License.

not rated for temperatures >300°C (Baron and Ungemach, 1981). During the test, a well-head pressure P_{tot} of 69.6 bar-a and a well-head temperature of 222°C were measured, at the same time. At 222°C and pure water saturation, P_{H_2O} is 24.1 bar, from the Steam Tables (Lemmon et al., 2023), and $P_{tot} - P_{H_2O} \cong P_{CO_2}$ is 45.5 bar, assuming that CO_2 is by far the main non-condensable gas constituent. Furthermore, the X_{H_2O} and X_{CO_2} of the gas phase at well head are 24.1 bar/69.6 bar = 0.35 and 45.5 bar/69.6 bar = 0.65, based on the Dalton's law. Summing up, previous considerations mainly based on the results of the AGIP-ENEL geothermal exploration suggest what follows:

(i) The supercritical gas phase rich in H_2O and CO_2 accumulates in volcanic and marine deposits strongly affected by thermometamorphic alteration below a quartz-rich caprock. The top of this relatively deep reservoir of supercritical fluids is found at ~2.8 km depth, while its areal extension coincides with the inner caldera block, marked by the gravimetric low, and the ground deformation area (Fig. 4).

(ii) It is likely that the pressurization of the ~2.8-km-deep reservoir of supercritical fluids is the "engine" of the ground uplift begun in 2006, also accompanied by anomalous shallow seismicity and increase in fumarolic emission.

(iii) Since the Solfatara-Pisciarelli fumarolic area is found near the center of the inner caldera block, it could be a sort of "exhaust valve" of the ~2.8-km-deep reservoir. This discussion is resumed in section 4.4.

4.2 The zone of CO equilibration

Considering that the total fluid pressure of CO equilibrium remained ~25 bar during the last 38 years and assuming that it is balanced by an external pressure of the same value, it can be inferred that CO equilibrium is attained in a shallow reservoir whose top is located at ~250 m depth. This depth agrees with that of the bottom of the low-resistivity, clay-rich caprock present below the Solfatara crater as indicated by audiomagnetotellurics (Siniscalchi et al., 2019). The shallow reservoir is assumed to correspond with the relatively conductive unit (10-30 Ω·m) which is situated below the caprock and has an average thickness of ~200 m. The areal extension of the shallow reservoir corresponds to that of the Solfatara diffuse degassing structure, ~1 km^2, as indicated by high CO_2 fluxes (Cardellini et al., 2017; Fig. 1b) and occurrence of advanced argillic alteration (Piochi et al., 2015).

4.3 Equilibrium versus disequilibrium between CO and CH_4

The disequilibrium between CO and CH_4 is a very likely condition in hydrothermal-magmatic environments, especially when the residence time of the fluid in the system is relatively short, because CO is a fast-reacting species and CH_4 is one of the slowest species to react (e.g., Giggenbach 1987). This does not exclude that equilibrium between CO and CH_4 can be reached, if the residence time of the fluid in the system is long enough. Actually, both conditions occurred, at different times, in the shallow reservoir below the Solfatara. In fact, CO- and CH_4 equilibrium temperatures were similar to each other, within

https://doi.org/10.5194/egusphere-2024-1306
Preprint. Discussion started: 22 May 2024
© Author(s) 2024. CC BY 4.0 License.

uncertainties, until July 1984, while the difference between the two temperatures increased more and more in the following years (Fig. 2). The attainment of CO-CH_4 equilibrium at the same temperature, pressure conditions was possible, until July 1984, because of the relatively long residence time in the shallow reservoir that received a nil to negligible inflow of deep gases from below and behaved as a closed system or nearly so, at that time, as proposed in the conceptual model of Cioni et al. (1984). The shallow reservoir opened in July-September 1984 and was affected, in the following years, by a time-increasing inflow of deep fluids, mostly coming from a degassing magma batch, as postulated by the conceptual model of Caliro et al. (2007) and adopted in the subsequent studies of Chiodini and coworkers. The change from closed to open state of the Solfatara magmatic-hydrothermal system explains the differences between the two models, that are both valid because they refer to two distinct time lapses.

Therefore, it is advisable to use reaction (1), involving CO but not CH_4, and reaction (2), including CH_4 but not CO, for geothermometric-geobarometric purposes. In other terms, it is better to consider CO and CH_4 separately, rather than using the following reaction:

$$CO + ½\ H_2O = ¾\ CO_2 + ¼\ CH_4, \quad (5)$$

as it involves both gas species with different stoichiometric coefficients, 1 for CO and ¼ for CH_4. Thus, in case of CO-CH_4 disequilibrium, the equilibrium temperature is meaningless as it is the weighted average of the CO- and CH_4 equilibrium temperatures given by reactions (1) and (2), respectively. Similar considerations apply to equilibrium pressures. Unfortunately, irrespective of these issues, reaction (5), together with reaction (1), was taken into account in several studies, including those carried out by Cioni and coworkers and Chiodini and coworkers for the Solfatara hydrothermal-magmatic system.

4.4 The zone of CH_4 equilibration

Owing to the sluggish behavior of CH_4, some geochemists, including Chiodini and coworkers, consider that it is a tracer instead of an indicator, as recalled above, whereas Moretti et al. (2017) treated CH_4 as a reactive species. To solve this dilemma, it must be noted that there is a good agreement between the CH_4 equilibrium temperature given by reaction (2) and the temperature of isotopic CH_4-CO_2 equilibrium, in spite of the limited number of isotope data available for the Solfatara fluids (Caliro et al., 2007; Fiebig et al., 2013, 2015). Assuming that this agreement is not fortuitous, it is legitimate to conclude that reaction (2) provides meaningful geothermometric results, at least for the Solfatara magmatic-hydrothermal system. Nevertheless, the depth of the reservoir where CH_4 and CO_2 equilibrate chemically and isotopically remains a matter of discussion. Since the attainment of this condition requires a time interval long enough, that is, the residence of the fluid into a sufficiently large reservoir, a possible candidate is the ~2.8-km-deep reservoir, whose areal extension coincides with that of the inner caldera block (Fig. 4; see section 4.1). Further information on this reservoir of supercritical fluids is provided by modeling of both the active seismic reflection data of the SERAPIS survey (Zollo et al., 2003; Judenherc and Zollo 2004; Zollo et al., 2008) and the passive seismic data of the 1982-1984 bradyseismic crisis (Vanorio et al., 2005; Chiarabba and Moretti 2006; Battaglia et al., 2008; De Siena et al., 2017), indicating that it extends from 2.7 to 4 km depth.

https://doi.org/10.5194/egusphere-2024-1306
Preprint. Discussion started: 22 May 2024
© Author(s) 2024. CC BY 4.0 License.

Recalling the available geological knowledge (section 4.1), the 2.7-4 km deep reservoir is covered by an impermeable layer generated by self-sealing, chiefly quartz deposition, at temperature of ~400°C, an important detail in line with the general conceptual model of volcano-hosted magmatic-hydrothermal systems of Fournier (1999). According to the Fournier's model, the quartz-rich layer separates: (a) the underlying deep-magmatic domain, where hypersaline brines and gases exsolved from the underlying crystallizing magma accumulate at lithostatic pressure within a volume of plastic rocks, from (b) the overlying shallow-hydrothermal domain, where hydrothermal fluids of meteoric and/or marine origin circulate through brittle rocks at hydrostatic pressure. Fournier (1999) also recognized that the quartz-rich self-sealed layer is broken, from time to time, by an uprise of magma or other processes determining the fast spill of hypersaline brines and gases from the plastic-magmatic domain into the brittle-hydrothermal domain, at smaller pressure and temperature. The resultant increase in fluid pressure and temperature within the brittle-hydrothermal domain triggers faulting and fracturing, with an ensuing increase in permeability and the discharge rate of magmatic–hydrothermal fluids. The Fournier's model is perfectly applicable to the Solfatara magmatic-hydrothermal system, as already recognized by other authors (e.g., Lima et al., 2009, 2021; Smale 2020; Kilburn et al., 2023), and allows us to understand both its structure and its evolution over time.

4.5 The zone of H_2S equilibration

The occurrence of reaction (3) is supported by the widespread presence of calcite and anhydrite veins in the carbonate-evaporite geothermal systems of Central Italy (Marini and Chiodini 1994), such as Latera, where both anhydrite and calcite are very abundant authigenic minerals also in the contact-metasomatism paragenesis (Cavarretta et al., 1985), that is, near the magma chamber. The Mesozoic carbonate sequence crops out all around the Campanian Plain, but it is found at depths greater than ~4 km in the Campi Flegrei, based on the evidence provided by seismic data (Zollo et al., 2008), whereas a melt zone occurs at depths of ~8.0 to ~8.5 km. Assuming the presence of a level of skarn and marble separating the two units, the carbonate sequence is expected to be situated from ~ 4 km to ~7.5 km depth. Thus, the H_2S equilibrium temperature is assumed to mark the base of the carbonate sequence, where the acidic fluids released from the underlying degassing magma are quickly neutralized through interaction with carbonate minerals, at depths of 6.5–7.5 km, to be considered as an educated guess.

The external (overburden) pressure at this depth is expected to be of 1330±135 bar, as indicated by the strip of sky-blue color in Fig. 3. Interestingly, in June 1983–July 1984, total fluid pressure at 6.5–7.5 km depth balanced the external pressure and the fluids present at the base of the carbonate sequence could not flow upward, in line with the conceptual model of Cioni et al. (1984; see above). Then, since September 1984, fluid pressure started to exceed the external pressure, although the difference between the fluid pressure and the overburden pressure remained relatively small until 2000-2001. A continuous and considerable increase in fluid pressure occurred afterwards and it was particularly important since 2016. This growth in the fluid pressure at 6.5–7.5 km depth with time explains the provenance of fumarolic fluids from the deep-magmatic portion of the Solfatara magmatic-hydrothermal system since September 1984, in agreement with the conceptual model of Caliro et al.,

https://doi.org/10.5194/egusphere-2024-1306
Preprint. Discussion started: 22 May 2024
© Author(s) 2024. CC BY 4.0 License.

(2007; see above), as well as the increasing degassing process observed at the surface (Chiodini et al., 2021 and references therein).

The H_2S equilibrium temperature can approach but cannot overcome 1120 °C, the temperature of the trachybasaltic magma present at depth (Caliro et al., 2014). Consistent with this expectation, the maximum computed H_2S equilibrium temperatures are 1040°C, for the Bocca Grande sample collected on October 8, 2019, and 1087°C, for the Bocca Nuova fluid sampled on September 1, 2020.

The CH_4 concentration at the H_2S equilibrium temperature has average of 0.00571±0.00194 (1σ) μmol/mol and range of 0.00355-0.0137 μmol/mol for Bocca Grande and average of 0.00429±0.00163 (1σ) μmol/mol and range of 0.00211-0.0171 μmol/mol for Bocca Nuova. These very small CH_4 concentrations are not surprising for magmatic fluids somewhat modified by absorption in deep brines and interaction with carbonate rocks. Consequently, it can be inferred that most CH_4 discharged at the surface is generated through different reactions, such as (2) and (5), upon cooling-depressurization of the gas mixture leaving the zone of H_2S equilibration, and adjustment to the final equilibrium value in the reservoir of supercritical fluids situated at depths of 2.7-4 km.

4.6 The revised conceptual model of the Solfatara magmatic-hydrothermal system

Based on previous discussion, we revised the conceptual model of the Solfatara magmatic-hydrothermal system, which is consistent with the geological-geophysical context of the Campi Flegrei and the hydrothermal mineralogy, both present at the surface in the Solfatara crater (Piochi et al., 2015) and encountered by deep geothermal wells (Chelini and Sbrana 1987). It includes the following units (from top to bottom):

(1) The cap-rock of the shallow reservoir (0-0.25 km depth) constituted by volcanic deposits affected by advanced argillic alteration, near the surface, and by argillic alteration far from it. Its areal extension corresponds to that of the Solfatara diffuse degassing structure.

(2) The shallow reservoir (0.25-0.45 km depth) hosted in volcanic deposits. It is a steam and gas pocket with areal extension of ~1 km^2, matching that of the Solfatara diffuse degassing structure, and volume of ~0.2 km^3.

(3) An impermeable sequence (0.45-2.7 km depth) comprising pre- and post-caldera volcanic and marine deposits, affected by phyllitic alteration, in the upper part, and by propylitic alteration, in the lower portion, with an impermeable quartz-rich layer produced by self-sealing at the base. Since the propylitic alteration causes an extensive lithification of the primary materials, the lower portion of this sequence has brittle behavior, is prone to fracture, and could locally host small aquifers. The areal extension of this unit corresponds to the inner caldera block.

(4) The intermediate reservoir (2.7-4 km depth) hosted in volcanic and marine deposits affected by thermometamorphic alteration, determining a broad textural rearrangement of primary lithotypes. The intermediate reservoir is the source of ground uplift and associated shallow seismicity due to the presence of over-pressurized supercritical fluids. The areal extension of the

https://doi.org/10.5194/egusphere-2024-1306
Preprint. Discussion started: 22 May 2024
© Author(s) 2024. CC BY 4.0 License.

intermediate reservoir matches the inner caldera block. Nevertheless, it could be compartmentalized rather than a single aquifer, as suggested by the piecemeal collapse mechanism of the inner caldera (Capuano et al., 2013).

(5) A thick carbonate pile (4-6.5 km depth) acting as aquiclude probably due to nil to negligible fracturing and dissolution, by analogy with the geothermal well Nisyros-1 (Ambrosio et al., 2010).

(6) The deep reservoir (6.5-7.5 km depth) hosted in carbonate rocks affected by fracturing and dissolution-precipitation processes driven by magmatic fluids. Its lateral extension is expected to reflect that of the underlying melt zone.

(7) A deep aquiclude (7.5-8 km depth) constituted by skarn and marble, produced by metasomatic and thermometamorphic processes. The aquiclude behavior of skarn and marble is supported by their nil porosity (e.g., Kerrick, 1977).

(8) The melt zone (depths >8 km) storing a trachybasaltic magma (Caliro et al., 2014) and extending over the whole outer caldera.

4.7 Time changes of temperature and total fluid pressure below the Solfatara

A schematic graphical presentation of the evolution with time, between September 1984 and January 2022, of the temperatures and pressures present at different depths in the Solfatara magmatic-hydrothermal system is given by the temperature and total fluid pressure profiles of Figs. 5 and 6, respectively. The two graphs were prepared assuming that CO-, CH_4-, and H_2S-equilibrium temperatures (Table A1) and related total fluid pressures (Table A2) below the Solfatara refer to depths of 0.25-0.45 km, 2.7-4 km, and 6.5-7.5 km, respectively (see previous section), whereas the temperatures and pressures in the impermeable units are assumed to vary linearly with depth. The temperature and pressure at the surface were set equal to the measured Bocca Grande outlet temperature and the atmospheric value, respectively, whereas a constant temperature of 1120 °C and a constant pressure of 2879 bar were imposed at 8 km depth based on the characteristics of the trachybasaltic magma present below the Campi Flegrei (Caliro et al., 2014) and the results of magmatic degassing modeling performed using the model of Papale et al. (2006) on H_2O-CO_2 solubility in magmas (Marini et al., 2022).

The temperature and total fluid pressure profiles of Figs. 5 and 6, respectively, are expected to be encountered along a hypothetical vertical borehole drilled in the Solfatara crater to a total depth of 8 km. However, it must be recalled that the three reservoirs, where CO, CH_4, and H_2S equilibrate, are connected to each other by a deeply-extending faulted-fractured zone which attains a total depth of ~8 km and acts as conduit for the uprise of the fluids discharging at Solfatara-Pisciarelli. This faulted-fractured zone was activated during the final phase of the 1982-1984 seismic crisis, along tectonic trends already active in the past (Rosi and Sbrana, 1987), as suggested by the occurrence of low-magnitudo earthquakes at depths of 0-8 km (D'Auria et al., 2011). This fluid flow permits a very efficient advective heat transport from the magma to the surface. Nevertheless, based on the temperature profile along the hypothetical well, the heat transfer appears to be controlled by conduction, in the impermeable zones between the three reservoirs, as well as above the shallow reservoir and below the deep reservoir, and by convection, which keeps the temperature constant, in the three reservoirs.

Fig. 5 shows that the temperature of the shallow reservoir, where CO equilibrates, remained nearly constant with time, whereas a considerable temperature increase affected the intermediate and deep reservoirs, where CH_4 and H_2S equilibrate, respectively,

https://doi.org/10.5194/egusphere-2024-1306
Preprint. Discussion started: 22 May 2024
© Author(s) 2024. CC BY 4.0 License.

as already noted above. A possible temperature decrease occurred in the intermediate and deep reservoirs in 2021, after the peak value of 2020. In spite of the remarkable temperature increment in deep reservoir, this parameter remained well below the temperature of the underlying magma, at all times, indicating that the heat transfer from the magma to the overlying rocks has never been interrupted during the last 38 years.

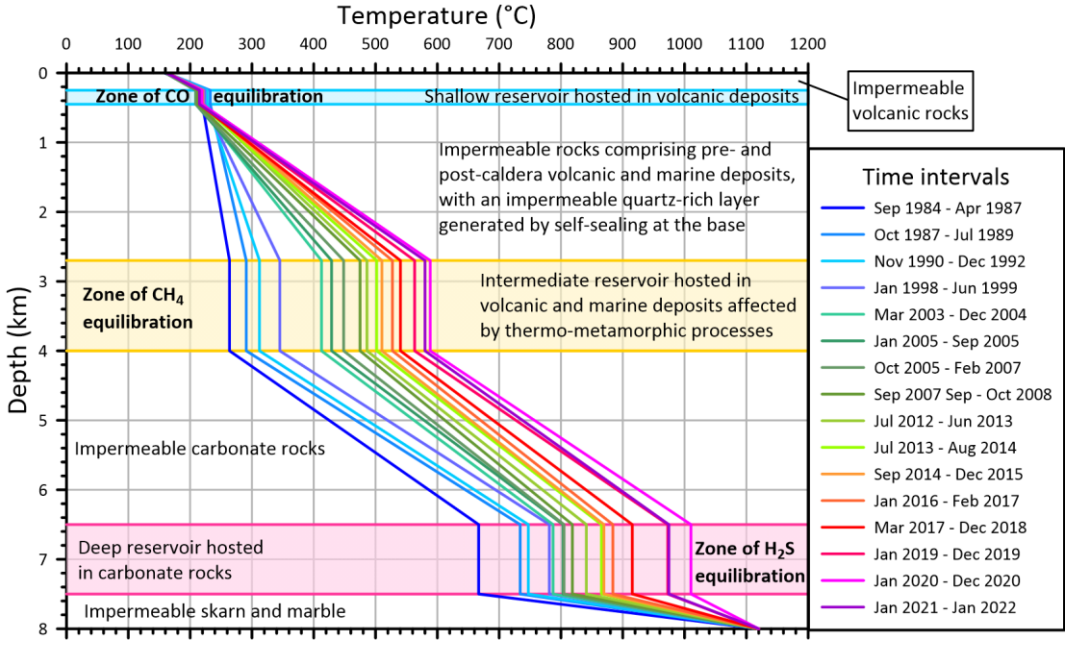

Figure 5. Time changes in September 1984-January 2022 of the temperature vs. depth profile along a hypothetical borehole drilled in the Solfatara crater. Also shown are the main lithological characteristics of the three reservoirs, where CO, CH_4, and H_2S equilibrate, and of the impermeable zones interposed between the three reservoirs, positioned above the shallow reservoir, and situated below the deep reservoir (see text for details).

The following observations can be drawn from Fig. 6: (a) As already noted above, the total fluid pressure of the shallow reservoir experienced nil to negligible changes with time whereas a remarkable pressurization, progressively increasing with time, impacted the intermediate and deep reservoirs. (b) In detail, the total fluid pressure in the deep reservoir became nearly equal to that of the underlying magma in 2019, exceeded it in 2020, and decreased in 2021 attaining again a value similar to that of the magma. So, the inflow of magmatic gases into the deep reservoir evidently stopped in the period 2019-2021, being prevented by pressures in the deep reservoir greater than or equal to the values of the underlying magma. The question is: how is it possible that total fluid pressure in the deep reservoir became equal to or even higher than that of the underlying magma? A possible explanation is the increasing rate, in 2019-2021, of the gas-producing reactions occurring in the deep reservoir, because of its continuous heating, with a consequent increase in the partial pressures of relevant gas species and in total fluid pressure. The most important of these gas-producing reactions is the decomposition of impure carbonate rocks, which is generally exemplified by the conversion of calcite and quartz to wollastonite and CO_2:

$$CaCO_3 + SiO_2 = CaSiO_3 + CO_2, \quad (6)$$

https://doi.org/10.5194/egusphere-2024-1306
Preprint. Discussion started: 22 May 2024
© Author(s) 2024. CC BY 4.0 License.

although other decarbonation reactions are possible (Marini, 2007) and probably occur in the considered system. Thus, the balance between the total fluid pressure in the deep reservoir and that of the underlying magma appears to be the "on-off switch" of magmatic degassing. (c) The total fluid pressure at the top of the shallow reservoir remained nearly equal to the external pressure in the entire time interval of interest (see section 4.2). In contrast, the total fluid pressure at the top of the intermediate reservoir became greater than the external pressure in the period March 2003-December 2004.

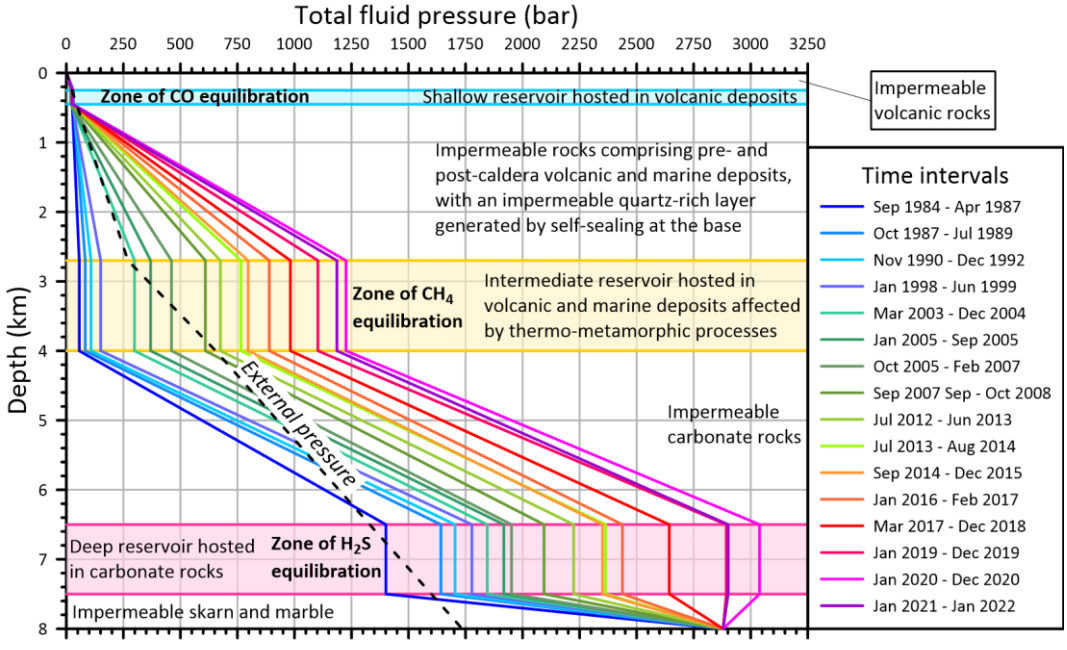

Figure 6. Time changes, between September 1984 and January 2022, of the total fluid pressure vs. depth profile along a hypothetical borehole drilled in the Solfatara crater. Also shown are (i) the main lithological characteristics of the three reservoirs, where CO, CH_4, and H_2S equilibrate, and of the impermeable zones interposed between the three reservoirs, positioned above the shallow reservoir, and situated below the deep reservoir (see text for details), as well as (ii) the external pressure gradient which is assumed to follow the hydrostatic regime above 2.7 km depth and the lithostatic regime below 4 km, with a transition zone between 2.7 and 4 km.

Disregarding isolated spikes and the frequent short-term fluctuations, the chronogram of the overpressure (the difference between total fluid pressure and external pressure) at the top of the intermediate reservoir (2.7 km depth; Fig. 7a) shows that the intermediate reservoir was not overpressurized before March 2003, whereas a general increase in the overpressure occurred afterwards, with a very weak decrease in 2007-2011 and a moderate decrease in 2020-2021.

The comparison of the chronogram of overpressure at 2.7 km depth with that of the vertical displacement at the center of the inner caldera (Fig. 7b) shows that there is a general correspondence between the two graphs and suggests that an overpressure of 200-250 bar is necessary to begin the ground uplift, the rate of which increases for higher overpressure values. Nevertheless, the two chronograms decoupled in 2021, when the overpressure decreased moderately but remained very high, with values of either 900-1000 bar or 1000-1150 bar based on Bocca Grande and Bocca Nuova data, respectively, whereas the positive

https://doi.org/10.5194/egusphere-2024-1306
Preprint. Discussion started: 22 May 2024
© Author(s) 2024. CC BY 4.0 License.

vertical movement continued, although with a somewhat lower rate, evidently because the overpressure was much higher than the initial threshold needed to push up the overlying rocks (see above). Moreover, in the biennium 2020-2021, the ground uplift was accompanied by an appreciable increment in the frequency of the shallow, low-magnitudo earthquakes occurring below the Solfatara area and in the adjacent sector of the Pozzuoli Gulf (Figs. 7c, 7d). These micro-seismic events were accompanied by a remarkable increase in the CO_2-rich gas flow from the Solfatara-Pisciarelli degassing structure, indicating the opening of new fractures in the rocks overlying the intermediate aquifer (Chiodini et al., 2021 and references therein) and the consequent increase in degassing from it. This, in turn, might be responsible of the moderate decrease in the overpressure at the top of the intermediate reservoir in 2020-2021. As expected on the basis of our conceptual model, the hypocenters of these earthquakes are found above the intermediate reservoir top (apart from a few cases) and within the inner caldera (see https://ingvvulcani.com/2023/09/09/lorigine-degli-sciami-sismici-ai-campi-flegrei-aggiornamento/ last access 24 April 2024).

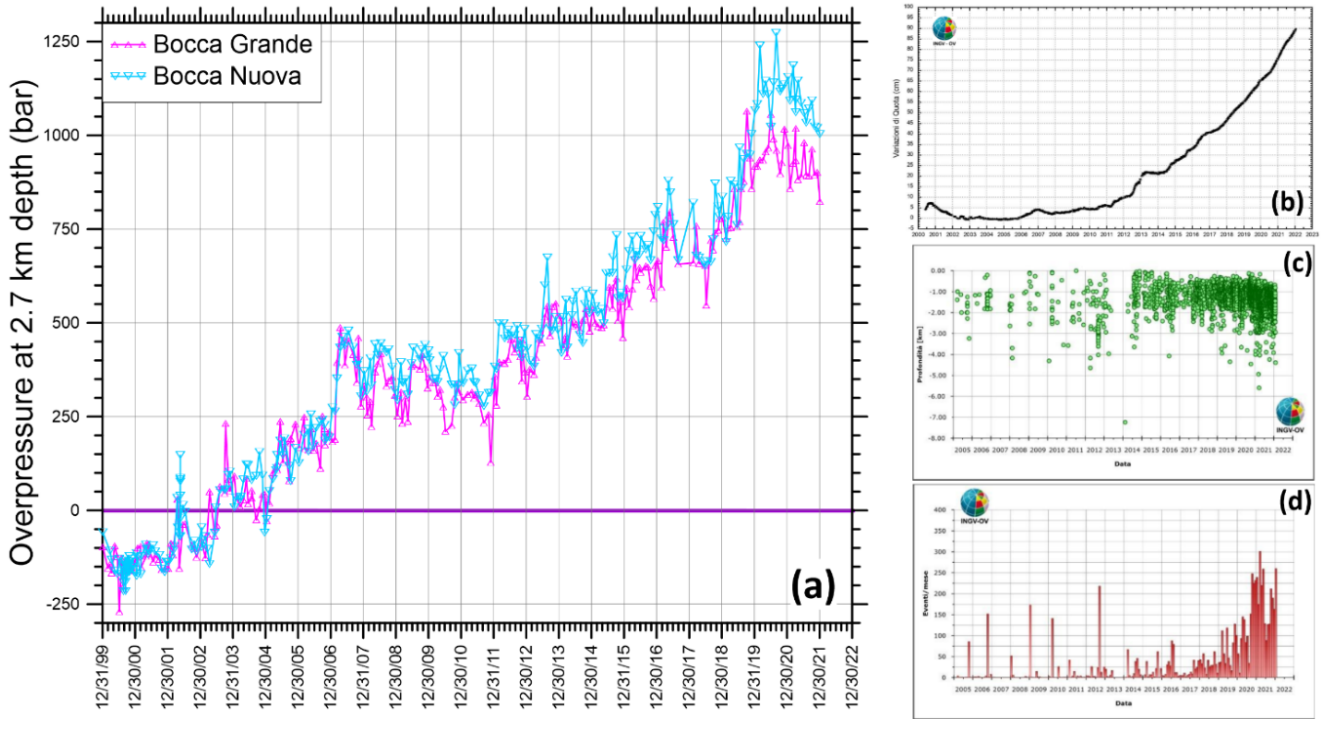

Figure 7. (a) Chronogram of the overpressure at the top of the intermediate reservoir (2.7 km depth), that is, the difference between the time-dependent total fluid pressure (computed from the chemistry of Bocca Grande and Bocca Nuova fumarolic fluids) and the constant external pressure, equal to 270 bar assuming a hydrostatic regime. Also shown are the chronograms of (b) the elevation at the center of the inner caldera, (c) earthquake depth, and (d) earthquake frequency (from INGV-Osservatorio Vesuviano, 2022). Elevation refers to benchmark 25A (leveling data for 1980–2009, Del Gaudio et al., 2010; GPS data for 2000–2020, RITE station, Pozzuoli – Rione Terra, Tramelli et al., 2021).

4.8 Possible future scenarios

Based on the revised conceptual model of the Solfatara magmatic-hydrothermal system described in section 4.6 and assuming the persistence of magmatic degassing and conductive heat transfer from the magma to the overlying rocks in the next future,

https://doi.org/10.5194/egusphere-2024-1306
Preprint. Discussion started: 22 May 2024
© Author(s) 2024. CC BY 4.0 License.

it is possible to make predictions on possible future scenarios. In this exercise, we assume the lack of external factors, such as the occurrence of one or more regional earthquakes and the input of fresh magma in the reservoir positioned at 8 km depth, two phenomena which may be related to each other and may trigger hydromagmatic and/or magmatic eruptions. We recall that the three reservoirs considered in the revised conceptual model are connected to each other by the deep-reaching fault-fracture zone that opened in the final phase of the 1982-1984 unrest episode.

For what concerns the deep reservoir, let us suppose that it is heated by conductive heat transfer from the underlying magma, but the inflow of magmatic fluids from below is prevented by the occurrence of decarbonation reactions maintaining the total fluid pressure at values higher than that of the magmatic fluids. This condition, which occurred in January 2019-January 2022, can persist over time if the conductive heat flux is high enough to sustain decarbonation reactions at a relatively high rate and ensure a sufficiently high fluid pressure in the deep reservoir. Alternatively, if the conductive heat flux is not high enough to sustain decarbonation reactions, the supply of magmatic fluid to the deep reservoir from below can be activated again, as occurred in September 1984-December 2018. Irrespective of the prevailing source of the deep fluids, they are doomed to leave the deep reservoir and flow upward, along the deep-reaching fault-fracture zone opened during the final phase of the 1982-1984 unrest episode, as long as their pressure is higher than that in the intermediate reservoir. This condition is expected to persist for a long time based on the nearly constant and high fluid pressure gradient between these two reservoirs in the whole period September 1984-January 2022. Nevertheless, possible changes due to internal factors cannot be excluded. For instance, calcite dissolution coupled with anhydrite precipitation according to the reverse of reaction (3) is expected to reduce the volume available to fluid circulation (Marini and Chiodini 1994) in the deep reservoir because the anhydrite molar volume at 25°C, 1 bar, 45.940 cm^3/mol, is much greater than that of calcite, 36.934 cm^3/mol, and the volume of solids changes little with temperature and pressure (Helgeson et al. 1978). Thus, in the long term, anhydrite deposition could clog pores and fractures at the base of the deep reservoir reducing or even stopping the supply of magmatic fluids from below.

Focusing on the intermediate reservoir, its fluid pressure and temperature are regulated by the balance between the flow of magmatic-thermometamorphic fluids entering it from below and the flow of fluids leaving it from the top, where the quartz-rich seal was broken in the 80's. The time-increasing seismic activity at depths <2.7 km during the last years has probably increased the flow of fluids out of the reservoir with a consequent decrease in the overpressure in 2021. Nevertheless, the ground uplift has continued, although with a lower rate, because the overpressure was still much higher than the threshold of 200-250 bar which appears to be needed to start the process (see previous section). If the decline in the overpressure will continue in the future, a gradual decrease in the rate of ground uplift is expected until the threshold of 200-250 bar is attained. A further decrease in the overpressure will lead first to stop and second to invert the ground movement.

Considering the shallow reservoir, its low temperature, ~220°C, and total fluid pressure, ~25 bar, and the constancy of these two parameters over time indicate that it has not been influenced by heating and pressurization, so far. The same inference can be drawn based on the somewhat higher temperature and pressure values of the shallow reservoir computed by Chiodini et al. (2021) using the CO/CO_2 geothermometers (see footnote 1 in section 3). However, the opening of new fractures in the rocks interposed between the intermediate aquifer and the shallow aquifer (which are progressively weakened by repeated

https://doi.org/10.5194/egusphere-2024-1306
Preprint. Discussion started: 22 May 2024
© Author(s) 2024. CC BY 4.0 License.

earthquakes) could cause a sudden upwards transfer of fluids, the pressurization of the shallow reservoir, and possibly a hydrothermal eruption.

Moreover, it cannot be excluded that, in an unknown future, the Solfatara magmatic-hydrothermal system may be affected by external events, such as the ascent of magmatic masses possibly triggered by one or more regional earthquakes, but it is not possible to forecast a priori the timing and the location of such extremely important events, whose detection is, in fact, the objective of the multidisciplinary, high-quality surveillance activities carried out by INGV.

5 Conclusions

The results of the new geothermometers and geobarometers (Marini et al., 2022) and the available geological, volcanological, and geophysical information allowed us to revise the conceptual model of the Solfatara magmatic-hydrothermal system. This revised model adds further details to the model of Caliro et al. (2007) and extends it at magmatic depth. Based on this revised conceptual model, it was possible: (1) to monitor the temperature and total fluid pressure over a large time interval in the reservoir present at shallow depth below the Solfatara, in the intermediate reservoir present at 2.7-4 km depth in the inner Campi Flegrei caldera, at least in the compartment below the Solfatara, and in the deep reservoir probably extending over the whole outer Campi Flegrei caldera, (2) to explain the evolution of pressurization-depressurization in the intermediate reservoir, acting as the "engine" of bradyseism, and the time changes of total fluid pressure in the deep reservoir, acting as the "on-off switch" of magmatic degassing, and (3) to make predictions on possible future scenarios of the Solfatara magmatic-hydrothermal system in the lack of external factors, such as the occurrence of regional earthquakes and the input of fresh magma in the reservoir at 8 km depth.

We underscore that the achievement of these results has been possible thanks to the availability of a large geochemical database, extending over 40 years, generated in the framework of volcanic surveillance, and a very large multidisciplinary geological, volcanological, and geophysical information obtained not only from surface investigations but also from the deep geothermal wells drilled by AGIP-ENEL in the '70s and '80s.

In future studies, the CO, CH_4, and H_2S temperatures and total fluid pressures at different times could be used to calibrate the numerical models for simulating the coupled transport of fluids and heat in the porous and fractured media present under the Solfatara crater, improving those developed in previous studies (e.g., Todesco, 2009). The temperatures and total fluid pressures in the shallow, intermediate and deep reservoirs at different times should also be considered to predict the rheological behavior of relevant rocks in the system of interest, thus ameliorating the results of previous investigations (e.g., Kilburn et al., 2023). Thermo-poro-elastic models (e.g., Nespoli et al., 2023) could also be improved taking into account the time changes of the temperatures and total fluid pressures in the intermediate reservoir computed by means of the gas-geoindicators of Marini et al. (2022).

If we want 500,000 people to continue to live in the Campi Flegrei area affected by the bradyseism without the sword of Damocles of a hydrothermal event, it is necessary to find an appropriate solution such as to guarantee the seismic stability of

https://doi.org/10.5194/egusphere-2024-1306
Preprint. Discussion started: 22 May 2024
© Author(s) 2024. CC BY 4.0 License.

a large number of buildings or to manage the bradyseism by zeroing the inflation of the intermediate reservoir depressurizing it. The first approach requires an investment without any economic return and does not mitigate the hazard posed by hydrothermal events. The second strategy provides a permanent solution to the problem in that it cancels the hazard posed by hydrothermal events. It requires a considerable initial investment to drill a suitable number of geothermal wells to depths of 3000-4000 m and to construct both a geothermal power plant and a mineral recovery plant. However, it provides a considerable economic return, thanks to the exploitation of geothermal energy for electrical production and the recovery of raw materials of utmost interest such as lithium. The feasibility of geothermal exploitation was proven by AGIP-ENEL activities carried out in the '70s and '80s (see above). The obstacles that existed at that time and caused the end of geothermal exploration no longer exist today, thanks to the improvements in drilling materials and technologies, as demonstrated by ongoing drilling activities in several supercritical geothermal systems (e.g., Reinsch et al., 2017).

Appendix A

Table A1. Average and standard deviations values of the outlet temperature, and CO-, CH_4-, and H_2S equilibrium temperatures for 24 selected time intervals, from June 1983 to January 2022, for the fumarolic samples collected at Bocca Grande by Cioni and coworkers and Chiodini and coworkers (data from Buono et al., 2023 and references therein).

Time interval	Outlet T (°C)		CO equil. T (°C)		CH_4 equil. T (°C)		H_2S equil. T (°C)	
	average	std.dev.	average	std.dev.	average	std.dev.	average	std.dev.
1983 Jun - 1984 Jul	156.9	0.6	227	13	246	8	667	24
1984 Sep - 1987 Apr	158.4	2.5	220	11	264	21	667	35
1987 Oct - 1989 Jul	162.0	0.0	233	10	291	26	734	12
1990 Nov - 1992 Dec	162.0	0.0	228	10	312	13	747	13
1993 Dec - 1995 Apr	162.2	0.6	208	21	302	17	709	9
1995 May - 1997 Dec	162.0	0.0	219	13	328	18	732	18
1998 Jan - 1999 Jun	161.8	0.9	224	5	345	21	781	21
1999 Aug - 2001 Mar	157.4	4.0	222	8	339	33	750	25
2001 Mar - 2003 Feb	159.8	1.2	219	7	356	29	759	14
2003 Mar - 2004 Dec	162.0	1.2	212	6	413	15	787	12
2005 Jan - 2005 Sep	159.9	2.2	209	3	429	17	803	14
2005 Oct - 2007 Feb	160.1	3.4	209	4	448	7	805	9
2007 Mar - 2007 Jul	161.0	1.4	208	6	498	8	815	18
2007 Sep - 2008 Oct	162.4	1.1	212	6	475	13	819	17
2008 Nov - 2010 Sep	163.0	0.9	215	7	470	12	813	11
2010 Oct - 2012 Jun	163.1	1.4	218	6	468	14	830	15
2012 Jul - 2013 Jun	163.2	1.1	220	5	486	10	841	12
2013 Jul - 2014 Aug	163.7	0.9	217	3	502	7	866	11
2014 Sep -2015 Dec	162.6	0.7	221	3	510	8	869	13
2016 Jan - 2017 Feb	163.6	0.6	220	3	527	8	884	16
2017 Mar - 2018 Dec	163.3	0.7	215	3	540	12	915	23

https://doi.org/10.5194/egusphere-2024-1306
Preprint. Discussion started: 22 May 2024
© Author(s) 2024. CC BY 4.0 License.

Time interval	Outlet T (°C)		CO equil. T (°C)		CH_4 equil. T (°C)		H_2S equil. T (°C)	
	average	std.dev.	average	std.dev.	average	std.dev.	average	std.dev.
2019 Jan - 2019 Dec	161.9	0.9	218	3	563	16	973	29
2020 Jan - 2020 Dec	161.9	1.2	219	3	589	8	1010	14
2021 Jan - 2022 Jan	162.4	1.2	215	3	580	8	975	23

Table A2. Average and standard deviations values of the CO-, CH_4-, and H_2S equilibrium pressures for 24 selected time intervals, from June 1983 to January 2022, for the fumarolic samples collected at Bocca Grande by Cioni and coworkers and Chiodini and coworkers (data from Buono et al., 2023 and references therein).

Time interval	CO equil. P (bar)		CH_4 equil. P (bar)		H_2S equil. P (bar)	
	average	std.dev.	average	std.dev.	average	std.dev.
1983 Jun - 1984 Jul	27.9	6.8	38.5	5.6	1308	102
1984 Sep - 1987 Apr	25.7	5.2	56.7	19.8	1401	184
1987 Oct - 1989 Jul	31.4	5.6	82.8	30.0	1642	58
1990 Nov - 1992 Dec	29.0	4.8	108	21	1704	81
1993 Dec - 1995 Apr	20.3	6.5	92.0	24.2	1491	36
1995 May - 1997 Dec	24.4	5.6	128	24	1619	73
1998 Jan - 1999 Jun	25.8	2.4	151	26	1778	82
1999 Aug - 2001 Mar	24.7	3.6	142	58	1645	106
2001 Mar - 2003 Feb	23.8	3.2	167	52	1696	64
2003 Mar - 2004 Dec	21.1	2.2	299	66	1845	57
2005 Jan - 2005 Sep	20.0	1.0	370	75	1918	69
2005 Oct - 2007 Feb	20.4	1.5	461	34	1951	42
2007 Mar - 2007 Jul	20.5	2.4	708	39	2042	71
2007 Sep - 2008 Oct	22.5	2.5	610	67	2094	76
2008 Nov - 2010 Sep	24.1	3.1	586	59	2073	57
2010 Oct - 2012 Jun	25.2	2.7	582	67	2157	67
2012 Jul - 2013 Jun	26.7	2.3	675	50	2224	59
2013 Jul - 2014 Aug	25.5	1.2	765	41	2364	57
2014 Sep -2015 Dec	27.1	1.2	797	44	2350	70
2016 Jan - 2017 Feb	27.0	1.5	890	40	2438	74
2017 Mar - 2018 Dec	25.5	1.3	982	65	2643	114
2019 Jan - 2019 Dec	27.1	1.3	1103	98	2893	160
2020 Jan - 2020 Dec	27.7	1.5	1226	46	3039	73
2021 Jan - 2022 Jan	25.6	1.3	1186	52	2901	120

Data availability

All raw data and results of geothermometers and geobarometers developed by Marini et al. (2022) are reported in Table S1.

https://doi.org/10.5194/egusphere-2024-1306
Preprint. Discussion started: 22 May 2024
© Author(s) 2024. CC BY 4.0 License.

Author contribution

ML wrote the geochemical aspects of the manuscript draft; CP wrote the geological aspects of the manuscript draft; LM reviewed and edited the manuscript.

Competing interests

The authors declare that they have no conflict of interest.

Acknowledgements

The Editors of the first and second journal we submitted our paper are warmly thanked for quickly reaching the decision that it was of no interest to their journals, in contrast with the Editor of the third journal who was unable to reach any conclusions in seven months, thus prompting us to withdraw our manuscript and submit it to Solid Earth.

References

Acocella, V.: Activating and reactivating pairs of nested collapses during caldera-forming eruptions: Campi Flegrei (Italy), Geophys. Res. Lett., L17304, https://doi.org/10.1029/2008GL035078, 2008.

Ambrosio, M., Doveri, M., Fagioli, M.T., Marini, L., Principe, C., and Raco, B.: Water–rock interaction in the magmatic-hydrothermal system of Nisyros Island (Greece), J. Volcanol. Geotherm. Res., 192, 57-68, https://doi.org/10.1016/j.jvolgeores.2010.02.005, 2010.

Barberi, F., Cassano, E., La Torre, P., and Sbrana, A.: Structural evolution of Campi Flegrei caldera in light of volcanological and geophysical data, J. Volcanol. Geotherm. Res. 48, 33-49, https://doi.org/10.1016/0377-0273(91)90031-T, 1991.

Baron, G. and Ungemach, P.: European geothermal drilling experience-Problem areas and case studies, US-DOE Office of Energy Efficiency and Renewable Energy Geothermal Technical Program, 24 pp., 1981.

Battaglia, J., Zollo, A., Virieux, J., and Dello Iacono, D.: Merging active and passive data sets in traveltime tomography: The case study of Campi Flegrei caldera southern Italy, Geophys. Prospect., 56, 555-573, https://doi.org/10.1111/j.1365-2478.2007.00687.x, 2008.

Bevilacqua, A., Neri, A., De Martino, P., Isaia, R., Novellino, A., Tramparulo, F.D.A., and Vitale, S.: Radial interpolation of GPS and leveling data of ground deformation in a resurgent caldera: application to Campi Flegrei (Italy), J. Geod., 94, 1-27, https://doi.org/10.1007/s00190-020-01355-x, 2020.

Bruni, P., Chelini, W., Sbrana, A., and Verdiani, G.: Deep exploration of the S. Vito area (Pozzuoli-NA) - well S. Vito 1, in: European Geothermal Update, edited by Strub, A.S. and Ungemach, P., Proceedings of the 3rd International Seminar on the Results of EC Geothermal Energy Research, Munich, Germany, 29 November-1 December, 1983, 390–406, 1985.

https://doi.org/10.5194/egusphere-2024-1306
Preprint. Discussion started: 22 May 2024
© Author(s) 2024. CC BY 4.0 License.

Buono, G., Caliro, S., Paonita, A., Pappalardo, L., and Chiodini, G.: Discriminating carbon dioxide sources during volcanic unrest: The case of Campi Flegrei caldera (Italy), Geology 51, 397-401, https://doi.org/10.1130/G50624.1, 2023.

Caliro, S., Chiodini, G., Moretti, R., Avino, R., Granieri, D., Russo, M., and Fiebig, J.: The origin of the fumaroles of La Solfatara (Campi Flegrei, south Italy), Geochim. Cosmochim. Ac., 71, 3040-3055, https://doi.org/10.1016/j.gca.2007.04.007, 2007.

Caliro, S., Chiodini, G., and Paonita, A.: Geochemical evidences of magma dynamics at Campi Flegrei (Italy), Geochim. Cosmochim. Ac., 132, 1-15, https://doi.org/10.1016/j.gca.2014.01.021, 2014.

Cardellini, C., Chiodini, G., Frondini, F., Avino, R., Bagnato, E., Caliro, S., Lelli, M., and Rosiello, A.: Monitoring diffuse volcanic degassing during volcanic unrests: the case of Campi Flegrei (Italy), Sci. Rep.-UK, https://doi.org/10.1038/s41598-017-06941-2, 2017.

Capuano, P., Russo, G., Civetta, L., Orsi, G., D'Antonio, M., and Moretti, R.: The active portion of the Campi Flegrei caldera structure imaged by 3-D inversion of gravity data, Geochem. Geophy. Geosy., 14, 4681-4697, https://doi.org/10.1002/ggge.20276, 2013

Cassano, E. and La Torre, P.: Geophysics, in: Phlegrean Fields, edited by: Rosi, M. and Sbrana, A., Quaderni de "La Scientifica", CNR, Roma, Italy, 114, vol. 9, 103–133, 1987

Cavarretta, G., Gianelli, G., Scandiffio, G., and Tecce, F.: Evolution of the Latera geothermal system II: metamorphic, hydrothermal mineral assemblages and fluid chemistry, J. Volcanol. Geotherm. Res., 26, 337-364, https://doi.org/10.1016/0377-0273(85)90063-0, 1985.

Chelini, W. and Sbrana, A.: Subsurface Geology, in: Phlegrean Fields, edited by: Rosi, M. and Sbrana, A., Quaderni de "La Scientifica", CNR, Roma, Italy, 114, vol. 9, 94-103, 1987.

Chiarabba, C. and Moretti, M.: An insight into the unrest phenomena at the Campi Flegrei caldera from Vp and Vp/Vs tomography, Terra Nova, 18, 373-379, https://doi.org/10.1111/j.1365-3121.2006.00701.x, 2006

Chiodini, G. and Marini, L.: Hydrothermal gas equilibria: The H_2O-H_2-CO_2-CO-CH_4 system, Geochim. Cosmochim. Ac., 62, 2673-2687, https://doi.org/10.1016/S0016-7037(98)00181-1, 1998.

Chiodini, G., Caliro, S., Avino, R., Bini, G., Giudicepietro, F., De Cesare, W., Ricciolino, P., Aiuppa, A., Cardellini, C., Petrillo, Z., Selva, J., Siniscalchi, A., and Tripaldi, S.: Hydrothermal pressure-temperature control on CO_2 emissions and seismicity at Campi Flegrei (Italy), J. Volcanol. Geotherm. Res., 414, 107245, https://doi.org/10.1016/j.jvolgeores.2021.107245, 2021.

Cioni, R., Corazza, E., and Marini, L.: The gas/steam ratio as indicator of heat transfer at the Solfatara fumaroles, Phlegraean Fields (Italy), B. Volcanol., 47, 295-302, https://doi.org/10.1007/BF01961560, 1984.

Cumming, W.: Geothermal resource conceptual models using surface exploration data, in: Proceedings of the 34th Workshop on Geothermal Reservoir Engineering, Stanford University, California, 9-11 February 2009, SGP-TR-187, 2009.

Cumming, W.: Resource conceptual models of volcano-hosted geothermal reservoirs for exploration well targeting and resource capacity assessment: Construction, pitfalls and challenges, Geoth. Res. T., 40, 623-637, 2016.

https://doi.org/10.5194/egusphere-2024-1306
Preprint. Discussion started: 22 May 2024
© Author(s) 2024. CC BY 4.0 License.

D'Amore, F. and Panichi, C.: Evaluation of deep temperature of hydrothermal systems by a new gas-geothermometer, Geochim. Cosmochim. Ac., 44, 549-556, https://doi.org/10.1016/0016-7037(80)90051-4, 1980

D'Auria, L., Giudicepietro, F., Aquino, I., Borriello, G., Del Gaudio, C., Lo Bascio, D., Martini, M., Ricciardi, G.P., Ricciolino, P., and Ricco, C.: Repeated fluid-transfer episodes as a mechanism for the recent dynamics of Campi Flegrei caldera (1989–2010), J. Geophys. Res.-Sol. Ea., 116, B04313, https://doi.org/10.1029/2010JB007837, 2011.

Deino, A.L., Orsi, G., de Vita, S., and Piochi, M.: The age of the Neapolitan Yellow Tuff caldera-forming eruption (Campi Flegrei caldera-Italy) assessed by $^{40}Ar/^{39}Ar$ dating method, J. Volcanol. Geotherm. Res., 133, 157-170, https://doi.org/10.1016/S0377-0273(03)00396-2, 2004.

Del Gaudio, C., Aquino, I., Ricciardi, G.P., Ricco, C., and Scandone, R.: Unrest episodes at Campi Flegrei: A reconstruction of vertical ground movements during 1905-2009, J. Volcanol. Geotherm. Res., 195, 48-56, https://doi.org/10.1016/j.jvolgeores.2010.05.014, 2010.

De Martino, P., Tammaro, U., and Obrizzo, F.: GPS time series at Campi Flegrei caldera (2000-2013), Ann. Geophys.-Italy, https://doi.org/10.4401/ag-6431, 2014.

De Siena, L., Chiodini, G., Vilardo, G., Del Pezzo, E., Castellano, M., Colombelli, S., Tisato, N., and Ventura, G.: Source and dynamics of a volcanic caldera unrest: Campi Flegrei, 1983–84, Sci. Rep.-UK., 7, 8099, https://doi.org/10.1038/s41598-017-08192-7, 2017.

Di Luccio, F., Pino, N.A., Piscini, A., and Ventura, G.: Significance of the 1982–2014 Campi Flegrei seismicity: Preexisting structures, hydrothermal processes, and hazard assessment, Geophys. Res. Lett., 42, 7498-7506, https://doi.org/10.1002/2015GL064962, 2015.

Fiebig, J., Tassi, F., D'Alessandro, W., Vaselli, O., and Woodland, A.B.: Carbon-bearing gas geothermometers for volcanic-hydrothermal systems, Chem. Geol., 351, 66-75, https://doi.org/10.1016/j.chemgeo.2013.05.006, 2013.

Fiebig, J., Hofmann, S., Tassi, F., D'Alessandro, W., Vaselli, O., and Woodland, A.B: Isotopic patterns of hydrothermal hydrocarbons emitted from Mediterranean volcanoes, Chem. Geol., 396, 152-163, https://doi.org/10.1016/j.chemgeo.2014.12.030, 2015.

Fournier, R.O.: Hydrothermal processes related to movement of fluid from plastic into brittle rock in the magmatic-epithermal environment, Econ. Geol., 94, 1193-1211, https://doi.org/10.2113/gsecongeo.94.8.1193,1999.

Giaccio, B., Hajdas, I., Isaia, R., Deino, A., and Nomade, S.: High-precision ^{14}C and $^{40}Ar/^{39}Ar$ dating of the Campanian Ignimbrite (Y-5) reconciles the time-scales of climatic-cultural processes at 40 ka, Sci. Rep.-UK., 7, 45940, https://doi.org/10.1038/srep45940, 2017.

Giggenbach, W.F.: Redox processes governing the chemistry of fumarolic gas discharges from White Island, New Zealand, Appl. Geochem., 2, 143-161, https://doi.org/10.1016/0883-2927(87)90030-8, 1987.

Guidoboni, E. and Ciuccarelli, C.: The Campi Flegrei caldera: historical revision and new data on seismic crises, bradyseisms, the Monte Nuovo eruption and ensuing earthquakes (twelfth century 1582 AD), B. Volcanol., 73, 655-677, https://doi.org/10.1007/s00445-010-0430-3, 2011.

https://doi.org/10.5194/egusphere-2024-1306
Preprint. Discussion started: 22 May 2024
© Author(s) 2024. CC BY 4.0 License.

Helgeson, H.C., Delany, J.M., Nesbitt, H.W., and Bird, D.K.: Summary and critique of the thermodynamic properties of rock-forming minerals, Am. J. Sci., 278A, 1-229, 1978.

INGV Osservatorio Vesuviano, Bollettino di Sorveglianza, Campi Flegrei, Gennaio 2022: https://www.ov.ingv.it/index.php/monitoraggio-e-infrastrutture/bollettini-tutti/flegrei/anno-2022-2/, last access 24 April 2024.

Isaia, R., Marianelli, P., and Sbrana, A.: Caldera unrest prior to intense volcanism in Campi Flegrei (Italy) at 4.0 ka BP: Implications for caldera dynamics and future eruptive scenarios, Geophys. Res. Lett., 36, L21303, https://doi.org/10.1029/2009GL040513, 2009.

Isaia, R., Vitale, S., Di Giuseppe, M.G., Iannuzzi, E., D'Assisi Tramparulo, F., and Troiano, A.: Stratigraphy, structure, and volcano-tectonic evolution of Solfatara maar-diatreme (Campi Flegrei, Italy), Geol. Soc. Am. Bull., 127, 1485-1504, https://doi.org/10.1130/B31183.1, 2015.

Judenherc, S. and Zollo, A.: The Bay of Naples (southern Italy): Constraints on the volcanic structures inferred from a dense seismic survey, J. Geophys. Res.-Sol. Ea., 109, B10312, https://doi.org/10.1029/2003JB002876, 2004.

Kerrick, D.M.: The genesis of zoned skarns in the Sierra Nevada, California, J. Petrol., 18, 144-181, https://doi.org/10.1093/petrology/18.1.144, 1977.

Kilburn, C.R., Carlino, S., Danesi, S., and Pino, N.A.: Potential for rupture before eruption at Campi Flegrei caldera, Southern Italy, Commun. Earth Environ., 4, 190, https://doi.org/10.1038/s43247-023-00842-1, 2023.

Lemmon, E.W., Bell, I.H., Huber, M.L., and McLinden, M.O.: Thermophysical Properties of Fluid Systems, NIST Chemistry WebBook, NIST Standard Reference Database # 69, https://webbook.nist.gov/chemistry/fluid/, last access 24 April 2024.

Lima, A., De Vivo, B., Spera, F.J., Bodnar, R.J., Milia, A., Nunziata, C., Belkin, H.E., and Cannatelli, C.: Thermodynamic model for uplift and deflation episodes (bradyseism) associated with magmatic–hydrothermal activity at the Campi Flegrei (Italy), Earth-Sci. Rev., 97, 44-58, https://doi.org/10.1016/j.earscirev.2009.10.001, 2009.

Lima, A., Bodnar, R.J., De Vivo, B., Spera, F.J., and Belkin, H.E.: Interpretation of recent unrest events (bradyseism) at Campi Flegrei, Napoli (Italy): Comparison of models based on cyclical hydrothermal events versus shallow magmatic intrusive events, Geofluids, 2021, 2000255, https://doi.org/10.1155/2021/2000255, 2021.

Lirer, L., Luongo, G., and Scandone, R.: On the volcanological evolution of Campi Flegrei, Eos T. Am. Geophys. Un., 68, 226-234, https://doi.org/10.1029/EO068i016p00226, 1987.

Lyell, C.: Principles of geology, 1st edition, vol. 1, John Murray, Albemarle-Street, London, 511 pp., https://library.si.edu/digital-library/book/principlesgeolovol1lyel, 1830.

Marini, L.: Geological Sequestration of Carbon Dioxide. Thermodynamics, Kinetics, and Reaction Path Modeling, Developments in Geochemistry, vol. 11, Elsevier, Amsterdam, The Netherlands, 453 pp., ISBN 9780444529503, 2007.

Marini, L. and Chiodini, G.: The role of carbon dioxide in the carbonate-evaporite geothermal systems of Tuscany and Latium (Italy), Acta Vulcanol., 5, 95-104, 1994.

https://doi.org/10.5194/egusphere-2024-1306
Preprint. Discussion started: 22 May 2024
© Author(s) 2024. CC BY 4.0 License.

Marini, L., Principe, C., and Lelli, M.: The Solfatara magmatic-hydrothermal system. Geochemistry, geothermometry and geobarometry of fumarolic fluids, Advances in Volcanology, Springer, Cham, Switzerland, 375 pp., https://doi.org/10.1007/978-3-030-98471-7, 2022.

Moretti, R., De Natale, G., and Troise, C.: A geochemical and geophysical reappraisal to the significance of the recent unrest at Campi Flegrei caldera (Southern Italy), Geochem. Geophy. Geosy., 18, 1244-1269, https://doi.org/10.1002/2016GC006569, 2017.

Nespoli, M., Tramelli, A., Belardinelli, M.E., and Bonafede M.: The effects of hot and pressurized fluid flow across a brittle layer on the recent seismicity and deformation in the Campi Flegrei caldera (Italy), J. Volcanol. Geotherm. Res., 443, 107930, https://doi.org/10.1016/j.jvolgeores.2023.107930, 2023.

Papale, P., Moretti, R., and Barbato, D.: The compositional dependence of the saturation surface of $H_2O + CO_2$ fluids in silicate melts, Chem. Geol., 229, 78-95, https://doi.org/10.1016/j.chemgeo.2006.01.013, 2006.

Piochi, M., Mormone, A., Balassone, G., Strauss, H., Troise, C., and De Natale, G.: Native sulfur, sulfates and sulfides from the active Campi Flegrei volcano (southern Italy): Genetic environments and degassing dynamics revealed by mineralogy and isotope geochemistry, J. Volcanol. Geotherm. Res., 304, 180-193, https://doi.org/10.1016/j.jvolgeores.2015.08.017, 2015.

Principe, C.: Managing different eruptive scenarios at Phlegraean Fields and Vesuvius, EGU General Assembly 2024, Online, 14–19 April 2024, EGU24-22302, https://doi.org/10.5194/egusphere-egu24-22302, 2024.

Principe, C., Rosi, M., Sbrana, A., and Zan, L.: Geological and gravimetric map of Phlegrean Fields at the 1:15,000 scale, in: Phlegrean Fields, edited by: Rosi, M. and Sbrana, A., Quaderni de "La Scientifica", CNR, Roma, Italy, 114, vol. 9, 1987.

Rittman, A.: Sintesi geologica dei Campi Flegrei, Boll. Soc. Geol. Ital., 69, 117-128, 1950.

Reinsch, T., Dobson, P., Asanuma, H., Huenges, E., Poletto, F., and Sanjuan, B.: Utilizing supercritical geothermal systems: a review of past ventures and ongoing research activities, Geotherm. Energy, 5, 16, https://doi.org/10.1186/s40517-017-0075-y, 2017.

Rosi, M., Sbrana, A., and Principe, C.: The Phlegraean Fields: structural evolution, volcanic history and eruptive mechanisms, J. Volcanol. Geotherm. Res., 17, 273-288, https://doi.org/10.1016/0377-0273(83)90072-0, 1983.

Rosi, M. and Sbrana, A.: Tectonics, in: Phlegrean Fields, edited by: Rosi, M. and Sbrana, A., Quaderni de "La Scientifica", CNR, Roma, Italy, 114, vol. 9, 80-93, 1987.

Siniscalchi, A., Tripaldi, S., Romano, G., Chiodini, G., Improta, L., Petrillo, Z., D'Auria, L., Caliro, S., and Avino, R.: Reservoir structure and hydraulic properties of the Campi Flegrei geothermal system inferred by audiomagnetotelluric, geochemical, and seismicity study, J. Geophys. Res.-Sol. Ea., 124, 5336-5356, https://doi.org/10.1029/2018JB016514, 2019.

Smale, L.: A re-interpretation of long-term deformation at Campi Flegrei caldera, Italy and perceptions of the causes of caldera unrest, Ph.D. thesis, Department of Earth Sciences, University College London, UK, 340 pp., 2020.

Todesco, M.: Signals from the Campi Flegrei hydrothermal system: Role of a "magmatic" source of fluids, J. Geophys. Res.-Sol. Ea., 114, B05201, https://doi.org/10.1029/2008JB006134, 2009.

https://doi.org/10.5194/egusphere-2024-1306
Preprint. Discussion started: 22 May 2024
© Author(s) 2024. CC BY 4.0 License.

Tramelli, A., Godano, C., Ricciolino, P., Giudicepietro, F., Caliro, S., Orazi, M., De Martino, P., and Chiodini, G.: Statistics of seismicity to investigate the Campi Flegrei caldera unrest, Sci Rep-UK, 11, 7211, https://doi.org/10.1038/s41598-021-86506-6, 2021.

Vanorio, T., Virieux, J., Capuano, P., Russo, G.: Three-dimensional seismic tomography from P wave and S wave microearthquake travel times and rock physics characterization of the Campi Flegrei Caldera. J. Geophys. Res.-Sol. Ea., 110, B03201, https://doi.org/10.1029/2004JB003102, 2005.

Zollo, A., Judenherc, S., Auger, E., D'Auria, L., Virieux, J., Capuano, P., Chiarabba, C., de Franco, R., Makris, J., Michelini, A., and Musacchio, G.: Evidence for the buried rim of Campi Flegrei caldera from 3-d active seismic imaging. Geophys. Res. Lett., 30, 2002, https://doi.org/10.1029/2003GL018173 , 2003.

Zollo, A., Maercklin, N., Vassallo, M., Dello Iacono, D., Virieux, J., and Gasparini, P.: Seismic reflections reveal a massive melt layer feeding Campi Flegrei caldera. Geophys. Res. Lett., 35, L12306, https://doi.org/10.1029/2008GL034242, 2008.